Characterization of supported cobalt and cobalt-rhodium catalysts. I. Temperature-programmed reduction (TPR) and oxidation (TPO) of Co---Rh/Al2O3

JOURNAL OF CATALYSIS 97, 188–199 (1986)

Characterization of Supported Cobalt and Cobalt–Rhodium Catalysts

I. Temperature-Programmed Reduction (TPR) and Oxidation (TPO) of $Co–Rh/Al_2O_3$

H. F. J. VAN 'T BLIK[1] AND R. PRINS[2]

Laboratory for Inorganic Chemistry, Eindhoven University of Technology, P.O. Box 513, 5600 MB Eindhoven, The Netherlands

Received August 14, 1984; revised June 26, 1985

Temperature-programmed reduction and oxidation (TPR and TPO) have been used to study the state of cobalt and rhodium in a series of $Co–Rh/\gamma\text{-}Al_2O_3$ catalysts. The results show that rhodium enhances the reducibility of part of the cobalt, but that it does not prevent the formation of cobalt aluminate, which is irreducible below 773 K. TPR of the coimpregnated $Co–Rh/\gamma\text{-}Al_2O_3$ catalyst shows a reduction peak at a much lower temperature than that of Co/Al_2O_3. This and the slight shift relative to the peak of Rh/Al_2O_3 indicates that cobalt and rhodium ions are not far apart after coimpregnation, which explains the easy formation of bimetallic particles during reduction. Passivation (oxidation at room temperature) of the reduced bimetallic catalyst leaves the structure of the bimetallic particles largely intact, but cobalt is oxidized to a great extent while rhodium remains metallic. Passivated Co–Rh particles thus consist of a rhodium kernel covered by cobalt oxide. TPR of passivated catalysts also suggests that already in the reduced state the bimetallic particles are surface-enriched in cobalt. A thorough oxidation of the bimetallic catalysts, on the other hand, leads to a restructuring, i.e., the formation of metal oxide particles which are in close proximity.

INTRODUCTION

Bimetallic catalysts are of interest for several industrial processes. The attractiveness of these catalysts lies in their superior stability and selectivity for many reactions (*1–3*). For example, Wise and co-workers (*4*) reported a maximum in selectivity for C_2 and C_3 hydrocarbons in Fischer–Tropsch synthesis for unsupported Fe–Co catalysts. Bhasin *et al.* (*5*) observed an increase in selectivity for methanol and ethanol in synthesis gas conversion over a bimetallic $Fe–Rh/SiO_2$ catalyst, compared with the supported monometallic catalysts.

In our laboratory we are interested in supported Co–Rh catalysts. Recently, Villeger *et al.* (*6*) have shown that addition of Rh to Co results in an increase of the selectivity to ethene and propene during CO hydrogenation. In order to understand the catalytic behavior of bimetallic catalysts the most fundamental question that has to be answered is whether the minute particles indeed contain atoms of both metals. On purely statistical grounds, one might expect the particles to be bimetallic. But direct experimental verification is difficult because of limitations in physical techniques.

The temperature-programmed reduction and oxidation techniques (TPR, TPO) may, however, be used to obtain evidence for the interaction between the atoms of the two metallic components. Thus, Robertson *et al.* (*7, 8*) were the first to study $Cu–Ni/SiO_2$ by means of TPR. They were able to confirm complete reduction and to identify alloying. Using TPR, evidence has also been found for an intimate contact between the constituent metals in $Pt–Re/Al_2O_3$ (*9*). In

[1] Present address: Philips Research Laboratories, P.O. Box 80.000, 5600 JA Eindhoven, The Netherlands.

[2] To whom correspondence should be sent.

0021-9517/86 $3.00

that study it was demonstrated that calcination of Pt–Re/Al_2O_3 at temperatures above 473 K caused segregation of platinum oxide and rhenium oxide. Paryjczak *et al.* (*10*) demonstrated the power of TPO in the characterization of bimetallic Rh–Ag/SiO_2 catalysts. The TPO profiles for these systems showed features intermediate between the characteristics of the pure components. Furthermore, it was found that the shape of the TPO profiles and the relative contributions of individual peaks depended on the degree of metal dispersion.

In this paper we present the results of a characterization study of the Co–Rh system supported on alumina by TPR and TPO. The formation of the bimetallic particles during reduction of the impregnated catalysts and their stability during oxidation will be discussed.

EXPERIMENTAL

The bulk metals Co and Rh and the bulk Co–Rh alloy with a Co/Rh atomic ratio of 1 were prepared by heating the corresponding aqueous solutions of the metal salts $Co(NO_3)_2 \cdot 6H_2O$ (Merck P. A.) and $RhCl_3 \cdot 3H_2O$ (39 wt%, Drijfhout) at 393 K, followed by a direct reduction of the resulting solid in hydrogen by heating at 5 K min^{-1} from room temperature to 1073 K and maintaining that temperature for 5 h. The monometallic bulk oxides Co_3O_4 and Rh_2O_3 were prepared by oxidizing the reduced metals at 1073 K for 72 h, while CoO was obtained from Merck. The mixed oxide $CoRhO_x$ was prepared by evaporating an aqueous solution of the metal salts followed by a direct oxidation at 1073 K (heating rate 5 K min^{-1}) for 48 h. γ-Al_2O_3 (Ketjen, 000-1.5 E, surface area 200 $m^2 g^{-1}$, pore volume 0.6 $cm^3 g^{-1}$) was (co)impregnated with aqueous solutions of the metal salts via the incipient wetness technique to prepare monometallic Co and Rh and bimetallic Co–Rh catalysts. The catalysts were dried in air at 393 K for 24 h after which a part of each batch was stored for further use. The other part was directly reduced in flowing H_2 by heating at 5 K min^{-1} to 773 K, maintaining that temperature for 1 h, and subsequently cooling in H_2 to room temperature. Thereafter, it was passivated at room temperature by replacing the H_2 flow by N_2 and subsequently slowly adding O_2 up to 20%. The Co and Rh contents of the dried catalysts were determined by using, respectively, atomic absorption spectroscopy and colorimetry. The catalysts which have been prepared are summarized in Table 1.

TABLE 1

Composition and Hydrogen Chemisorption Data for Alumina-Supported Co, Rh, and Co–Rh Catalysts

Catalyst	wt% Co	wt% Rh	H/M 773[a]	H/M[b]
Co/Al_2O_3	4.44		0.09	0.14
Co_4Rh/Al_2O_3	3.18	1.39	0.13	0.24
$CoRh/Al_2O_3$	1.97	3.43	0.39	0.57
Rh/Al_2O_3		2.30	1.53	
Rh/Al_2O_3		4.70	0.96	
Rh/Al_2O_3		8.53	0.81	

[a] Based on H_2 adsorption at room temperature after rereduction at 773 K.

[b] Dispersion of the metallic part of Co + Rh, corrected for the presence of $CoAl_2O_4$.

Hydrogen chemisorption measurements were carried out in a conventional volumetric glass apparatus after reduction of the passivated catalysts at 773 K (heating rate 5 K min^{-1}) in flowing hydrogen for 1 h, followed by evacuation at 773 K for Rh/Al_2O_3 and at 573 K for the cobalt-containing catalysts for another hour. The cobalt-containing catalysts were evacuated at lower temperatures in order to avoid formation of water by dehydroxylation of the support and thus to avoid reoxidation of cobalt (see Results). After evacuation, H_2 was admitted at 473 K, the catalyst was cooled to room temperature and desorption isotherms were measured at room temperature. The H/M value was obtained by extrapolating the linear higher pressure region ($P > 30$ kPa, above which monolayer coverage has been reached) of the isotherm to zero pressure and by subtraction of the contribution of the bare support. The H/Rh

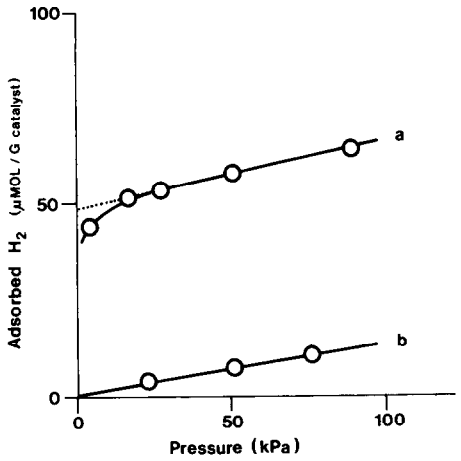

FIG. 1. Hydrogen chemisorption isotherms measured at 298 K for the 0.57 wt% Rh/Al_2O_3 catalyst. (a) Catalyst, (b) bare support.

values thus obtained for the various catalysts are presented in Table 1. A typical isotherm for a Rh catalyst is presented in Fig. 1.

TPR, TPO, and TPD experiments were carried out with 5% H_2 in Ar, 5% O_2 in He, and 100% Ar, respectively, with about 200 mg catalyst in an apparatus similar to that described by Boer *et al.* (*11*). The flow rate of gases through the reactor was 5 cm^3 min^{-1} and the temperature was raised at 5 K min^{-1} during TPR and TPO and at 15 K min^{-1} during TPD within the temperature range of 223 to 773 K.

The following typical sequence of treatments in the TPR apparatus has been used:

—the impregnated, passivated, or oxidized sample was flushed under Ar flow at 223 K;

—Ar was replaced by the Ar/H_2 mixture, causing at least an apparent H_2 consumption (first switch peak);

—the sample was heated under Ar/H_2 flow at 5 K min^{-1} to 773 K;

—after 1 h at 773 K the sample was cooled down at 10 K min^{-1} to 223 K;

—the reduced sample was flushed with Ar;

—Ar flow was replaced by the Ar/H_2 mixture once again, now causing only an apparent H_2 consumption (second switch peak). The difference between the first and second switch peak reveals the real hydrogen consumption at 223 K, if there is any (*12*).

A similar sequence has been followed during TPO, albeit that the final temperature was varied. When the TPR was followed by a TPO the TPR sequence was extended by heating the catalyst at 573 K for half an hour under helium flow, in order to desorb hydrogen, after which the catalyst was cooled down to 223 K again.

RESULTS AND DISCUSSION

Unsupported Bulk Co, Rh, and Co–Rh

It is known from the literature that Co and Rh are completely miscible (*13*). In Fig. 2 the X-ray diffraction (XRD) patterns (Cu$K\alpha$ radiation) are shown for a physical mixture of cobalt and rhodium, for the Co–Rh alloy, for a physical mixture of Co_3O_4 and Rh_2O_3, and for the mixed $CoRhO_x$ oxide. The diffraction pattern in Fig. 2a is formed by two peaks, the larger one being the (111) diffraction peak of rhodium with fcc structure and the smaller one the (111) diffraction peak of cobalt with fcc structure. From the 2θ values the Rh–Rh and Co–Co interatomic distances are calculated to be 2.688 and 2.505 Å, respectively. The

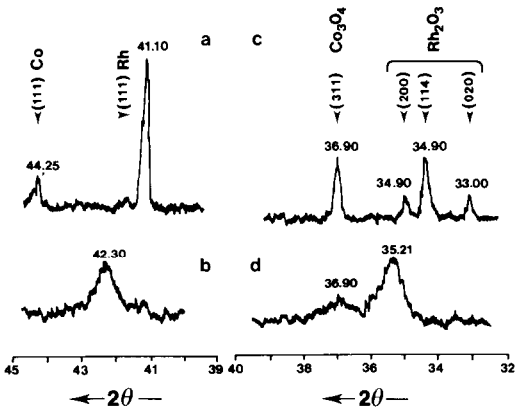

FIG. 2. X-Ray diffraction patterns (Cu$K\alpha$ radiation). (a) Physical mixture of metallic Co and Rh, (b) Co–Rh alloy (molar ratio is 1), (c) physical mixture of Co_3O_4 and Rh_2O_3, (d) $CoRhO_x$ mixed oxide.

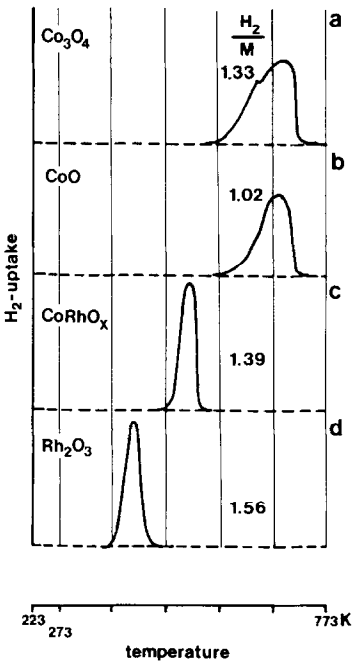

FIG. 3. TPR profiles for bulk oxides. (a) Co_3O_4, (b) CoO, (c) $CoRhO_x$, and (d) Rh_2O_3.

XRD pattern for the alloy (cf. Fig. 2b) shows a main peak at $2\theta = 42.30°$ which is in between the peaks of the constituent alloy components. No information is available about the crystallographic structure of the alloy, but assuming that its structure is fcc and that the peak is due to the (111) diffraction, the shortest metal–metal distance is on the average 2.615 Å. This value is slightly higher (0.017 Å) than predicted by Végard's rule (which assumes a linear relation between the interatomic distance in an alloy and the atomic ratio of the metals). Between $2\theta = 32°$ and 38° four diffraction peaks can be distinguished for the physical mixture of Co_3O_4 and Rh_2O_3 (Fig. 2c). The peaks at $2\theta = 33.00°$, 34.30°, and 34.90° are assigned to the (020), (114), and (200) diffractions of Rh_2O_3 (corundum structure), respectively, and the peak at $2\theta = 36.90°$ to the (311) diffraction of Co_3O_4 (spinel structure). The XRD pattern of the mixed $CoRhO_x$ oxide is characterized by two peaks (Fig. 2d). We assign the larger peak to a diffraction of $CoRh_2O_4$. This compound can be formed at 1073 K and higher temperatures (*14*) and is a normal spinel with Co^{2+} ions at tetrahedral positions and Rh^{3+} at octahedral positions. In the preparation of the mixed oxide we started with equimolar amounts of cobalt and rhodium salts, and therefore, besides $CoRh_2O_4$, another cobalt oxide must be present. The position of the weaker diffraction peak in Fig. 2d is equal to the one in Co_3O_4 (cf. Fig. 2c) and therefore we conclude that the residual cobalt was oxidized to Co_3O_4.

In order to obtain more insight into the reducibility of the bulk oxides we recorded TPR profiles of the different oxides diluted with Al_2O_3. The results are presented in Fig. 3. The numbers next to the TPR profiles correspond to the ratios of hydrogen consumed to the total amount of metal in moles. The reduction process of bulk Co_3O_4 and CoO does not start until 573 K (cf. Figs. 3a and b). It is seen that the profiles for the two bulk oxide samples are very similar, with peak maxima of 685 K for CoO and 703 K for Co_3O_4. However, for Co_3O_4 a second maximum at 648 K is observed. The two maxima for Co_3O_4 suggest a two-stage reduction process. This result is in satisfactory agreement with investigations carried out by Brown *et al.* (*15*) and Paryjczak *et al.* (*16*). However, the latter group observed a maximum of the main peak in the Co_3O_4 TPR profile at 673 K, which is 12 K lower than in our case. They even used a higher heating rate as well as a higher gas flow, which in general are known to induce a shift of the peak maximum to higher temperature (*17*). The observed H_2/M value of 1.02 for CoO is consistent with the theoretically expected value of 1.00. Note that the H_2 consumption in the TPR has been calibrated by means of Co_3O_4 (i.e., $CoO_{1.33}$). The TPR profile of bulk Rh_2O_3 is characterized by a sharp single peak at 408 K (Fig. 3d). The observed H_2/M value of 1.56 is equal to the theoretical value within experimental error.

The reduction of the oxidized Co–Rh al-

loy with an atomic Co/Rh ratio of 1 takes place within the temperature range of 453–523 K (Fig. 3c). According to the XRD results the mixed oxide consists of $CoRh_2O_4$ and Co_3O_4; the theoretical H_2/M value is therefore 1.33. Within the experimental error, the observed H_2/M value of 1.39 is in accordance with this. A striking feature is that the reduction profile is characterized by a sharp single peak. This indicates that the phase-separated Co_3O_4 is nevertheless in intimate contact with $CoRh_2O_4$ and that the latter serves as a catalyst for the reduction of Co_3O_4, because the Co_3O_4 is already completely reduced at a temperature at which it would just start to reduce without the presence of cobalt rhodate (cf. Fig. 3a).

Co, Rh, and Co–Rh Supported on γ-Al_2O_3

The hydrogen chemisorption results for Co, Rh, and Co–Rh on γ-Al_2O_3 are summarized in Table 1. The H/M values for a 4.70 and a 8.53 wt% Rh/γ-Al_2O_3 are also given. By a linear interpolation between these two values one obtains a value of H/M = 0.84 for a 7.75 wt% Rh catalyst. This loading corresponds to the same ratio of moles of metal to surface area of the support as for the monometallic cobalt catalyst, and dramatically demonstrates the high difference in dispersion of cobalt and rhodium on Al_2O_3. The high ratio of H/Rh = 1.53 for the 2.3 wt% Rh/Al_2O_3 catalyst has been commented upon in another publication (*18*). It can be clearly seen that the dispersion of the bimetallic catalysts increases with rhodium content. As described in the Experimental section, we admitted hydrogen at 473 K. Although, in contradistinction to rhodium, adsorption of hydrogen on cobalt is an activated process (*19*), we did not observe an effect of temperature on the ultimate amount of adsorption. However, adsorption was accelerated, and equilibrium was reached much faster.

TPR, TPO, and TPD profiles of the alumina-supported Co, Co_4Rh, and Rh catalysts are shown in Fig. 4. The numbers next to the profiles correspond to the ratio of the amount of gas consumed to the total amount of metal. Reduction of the 4.44 wt% Co/γ-Al_2O_3 catalyst after impregnation and drying occurs within the temperature range 443–653 K and is characterized by a single broad peak with its maximum at 543 K (Fig. 4a). The theoretical H_2/M value for the reduction of Co^{2+} to metallic Co is 1.00. The observed H_2/M value of 1.75 exceeds the theoretical value because of the simultaneous reduction of residual nitrate

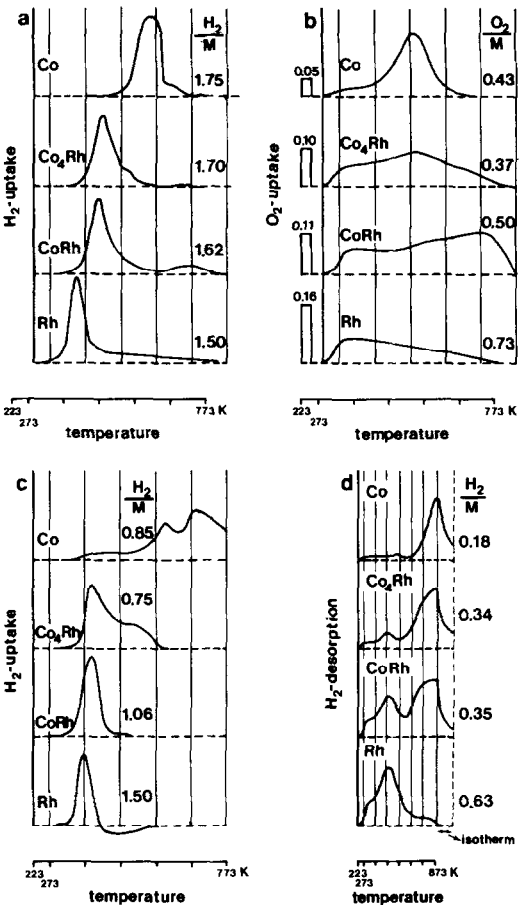

FIG. 4. TPR, TPO, and TPD profiles for alumina-supported Co (4.44 wt%), Co_4Rh (4.57 wt%), CoRh (5.40 wt%), and Rh (2.30 wt%) catalysts. (a) TPR of the impregnated and dried catalysts, (b) TPO of the reduced catalysts, (c) TPR of the oxidized catalysts, (d) TPD of the reduced catalysts, the metal particles of which are covered with hydrogen.

groups. The reduction of the impregnated and dried 2.30 wt% Rh/γ-Al_2O_3 catalyst already starts at 273 K (Fig. 4a). The TPR profile peaks at 363 K and has a weak tail up to 773 K. This peak is assigned to the reduction of well-dispersed $RhCl_3$, probably bound to the support in the form of —$(OH)_3$—$RhCl_3$ complexes (the hydroxyl groups of which belong to the support), or of hydrolyzed Rh^{3+} ions (*18*). The reduction behavior of these species might be similar to the one of passivated or oxidized highly-dispersed rhodium. No crystalline $RhCl_3$ is present because in that case the peak maximum would have been at about 413 K (*20*). As hydrogen consumption is only caused by the reduction of rhodium ions to metallic rhodium the observed H_2/M value of 1.50 indicates that the starting material was indeed in the +3 oxidation state.

A striking feature of the TPR profiles for the bimetallic catalysts is that the impregnated and dried Co_4Rh and CoRh supported catalysts are already reduced to a great extent before the reduction of the monometallic cobalt catalysts even starts. This indicates that the initiation of the reduction of the cobalt salt is aided by the presence of rhodium. The catalytic effect of rhodium can be explained by assuming that the very first formed metallic rhodium acts as a nucleation center. (Note that supported rhodium chloride is reduced before the reduction of cobalt nitrate starts.) At these sites hydrogen molecules are dissociated to yield hydrogen atoms which are more reactive in reduction than the molecules and consequently reduce the cobalt nitrate earlier. The maxima of the TPR profiles corresponding to the bimetallic systems are shifted to higher temperatures compared to the one of the impregnated monometallic rhodium catalysts. The shift is more pronounced with increasing cobalt content. The positions of the maxima are at about 413 K, the same temperature at which crystalline $RhCl_3$ is reduced. For the same reason as mentioned for the reduction of supported $Co(NO_3)_2$ the observed H_2/M values for both supported bimetallic catalysts cannot be used to determine the degree of reduction of the catalysts.

The TPR results demonstrate that the more noble metal Rh catalyzes the reduction of the salt of the less noble metal. For such a catalyzed reduction to take place, the metal salts should either be close together, or the reduced metal atoms must be able to diffuse over the support surface and aid in the reduction of the metal ions they encounter. Since cobalt and rhodium are completely miscible, it is logical to assume that bimetallic Co–Rh particles will be formed during reduction. On the other hand, an alternative explanation for the catalyzed reduction of the cobalt salt might be that hydrogen atoms are being spilled over from metallic rhodium particles to the support and that these hydrogen atoms reduce the cobalt ions. In that case, separate rhodium and cobalt particles might be formed. In the following we shall demonstrate, however, that the TPR profiles of passivated Co–Rh catalysts are different from those of monometallic Co or Rh catalysts (vide infra). This proves that metallic Co and Rh particles are not separately present on the support after reduction. Furthermore, we shall demonstrate in a subsequent publication on Co–Rh/SiO_2 catalysts that the EXAFS (Extended X-Ray Absorption Fine Structure) Rh K-edge spectrum shows that rhodium atoms in the reduced catalyst have rhodium as well as cobalt neighboring atoms (*21*). Because of the fact that part of the cobalt dissolves in the Al_2O_3 support (vide infra), this EXAFS experiment did not give unequivocal results for Co–Rh/Al_2O_3 catalysts. Furthermore, Mössbauer and ESR experiments on comparable Fe–Rh and Ni–Rh catalysts, respectively, demonstrated that also after reduction of these catalysts bimetallic (alloyed) catalysts were formed. Thus the Mössbauer spectrum of a Fe–Rh/SiO_2 catalyst showed a single peak due to alloyed Fe and no peaks of monometallic Fe (*22*), while ESR showed a strong peak due to superparamagnetic Ni in a re-

duced monometallic Ni/SiO_2 catalyst, and no ESR signal in a reduced $Ni–Rh/SiO_2$ catalyst. Apparently, alloying of Ni with Rh suppresses the Curie temperature substantially (*23*).

The hydrogen chemisorption results show that the dispersions of the bimetallic catalysts and the monometallic cobalt catalyst are significantly lower than that of the monometallic rhodium catalyst (cf. Table 1). This raises the intriguing question by what factors the dispersions of these catalysts are determined. We will first focus our attention on the monometallic systems. Beyond all doubt the interaction between cobalt and alumina is stronger than the interaction between rhodium and the support. It appears that in Co/Al_2O_3 cobalt always forms a cobalt spinel, possibly as an epitaxial layer between the γ-Al_2O_3 and the cobalt metal (*24*). Interactions based on interdiffusion of metal oxides with the oxidic support are strong. However, from the hydrogen chemisorption results it is clear that rhodium is much better dispersed on alumina than is cobalt. Although we must make a correction for the loss of cobalt metal caused by cobalt aluminate formation (see below), which when taken into account leads to an increase of the cobalt H/M value, the H/M value for the really metallic part of the monometallic cobalt catalyst will not exceed 0.20. The low dispersion can only be understood when it is assumed that before reduction the cobalt was poorly dispersed on alumina. This might be explained by sintering of cobalt oxide, which is formed by decomposition of $Co(NO_3)_2$ during drying of the impregnated catalyst. The change in color during drying of the impregnated catalyst from violet to black proves the decomposition of $Co(NO_3)_2$. Another explanation might be that no sites for the adsorption of cobalt ions are present. The pH of the aqueous solution of cobalt nitrate used for the impregnation is about 3, which means that the hydroxyl groups of the support are protonated to $—OH_2^+$. Therefore, the adsorption of cobalt ions which are present as $Co(H_2O)_6^{2+}$ in solution might be hindered by repulsion.

$RhCl_3$ does not suffer from adsorption problems because it is present as a neutral molecule $RhCl_3(H_2O)_3$ in an acidic aqueous solution, or even as an anionic chloride complex. An explanation for the relatively low H/M values observed for the bimetallic catalysts might be that during coimpregnation and drying the metal salts have not been homogeneously spread over the support. This view is supported by the TPR results. The TPR profiles obtained for the impregnated bimetallic catalysts peak at about the same temperature (413 K) as crystalline $RhCl_3$, whereas well-dispersed $RhCl_3$ gives rise to a TPR profile with a maximum at 363 K. Apparently, the presence of cobalt nitrate hinders the formation of a well-dispersed $RhCl_3$ phase on the alumina surface. During the impregnation a cobalt surface spinel ($CoAl_2O_4$) might be formed, through which a modification of the alumina surface occurs. Adsorption of $RhCl_3$ might then be hampered. It is obvious that the upper level of dispersion for a metal catalyst is already determined in an early stage of preparation with the choice of metal precursor.

The TPO profiles (Fig. 4b) of the four systems supported on alumina show oxygen consumption already at 223 K due to chemisorption. From the observed O_2/M values one can determine the degree of reduction of the catalyst after the first TPR by assuming that after oxidation Co_3O_4 and Rh_2O_3 are formed. Oxidation of the reduced monometallic cobalt catalyst already starts at 223 K and is complete at about 650 K. Maximum oxygen consumption takes place at 483 K. The observed O_2/M value of 0.43 indicates that the average oxidation state of cobalt after the first TPR, and before the TPO measurement, was +0.71. TPO profiles of a reduced 1.00 and a 2.02 wt% Co/γ-Al_2O_3 catalyst (not shown) displayed hardly any O_2 consumption. The average oxidation states of cobalt in these catalysts after reduction were calculated to be, respec-

tively, +2 and +1.9. The formation of $CoAl_2O_4$ in the three cobalt catalysts, mentioned above, after the first TPR and a subsequent passivation has been determined using UV reflectance spectroscopy. The $CoAl_2O_4$ signal hardly differed in intensity for these catalysts. Therefore, we conclude that after reduction of the 4.44 wt% Co/γ-Al_2O_3 catalyst $CoAl_2O_4$ as well as metallic cobalt were formed and that during the subsequent TPO only the metallic cobalt was oxidized to Co_3O_4. It is known that after calcination of a Co/Al_2O_3 catalyst several types of cobalt species exist on the catalyst surface: these are (i) a species resulting from diffusion of Co ions into tetrahedral lattice sites of γ-Al_2O_3 (often referred to as a "surface spinel" (*25*)), (ii) Co ions in octahedral sites of the support and/or (iii) "bulk-like" Co_3O_4.

The present results demonstrate that even after a direct reduction of the impregnated and dried cobalt catalyst a significant amount of the so-called "surface spinel" is formed. From the observed O_2/M value it is calculated that the amount of cobalt which had been converted to $CoAl_2O_4$ was 1.58 wt%.

The TPO profile recorded for the reduced 2.3 wt% Rh/γ-Al_2O_3 catalyst (Fig. 4b) is characteristic for an ultradispersed system. This has been discussed in a previous publication (*18*). The observed O_2/M value of 0.73 indicates that after the TPR run all rhodium was completely reduced and that all rhodium was oxidized to Rh_2O_3 during the TPO run. The TPO profiles for the two reduced bimetallic catalysts demonstrate that oxidation of the catalyst is more difficult with increasing rhodium content. The TPO profiles of the bimetallic catalysts resemble the TPO profile of an 11.64 wt% Rh/γ-Al_2O_3 catalyst with H/M = 0.67 (*18*). Two areas of oxygen consumption showed up in that profile, namely a peak around room temperature, attributed to corrosive chemisorption and one around 723 K, attributed to thorough oxidation, respectively (*18*). The dispersions of the bimetallic systems are lower than that of the 11.64 wt% Rh/γ-Al_2O_3 catalyst (see below). Since the latter shows the same TPO profile we assign the oxygen consumption above 573 K to thorough oxidation of rhodium.

From the observed O_2/M values, we cannot calculate the exact amounts of $CoAl_2O_4$ in the bimetallic catalysts formed after the first TPR, but upper and lower limits can be determined. On the basis of the TPR/TPO results obtained for the monometallic rhodium catalyst we assume that rhodium in the bimetallic system can be reduced to Rh^0 during TPR and completely oxidized to Rh_2O_3 during TPO. The upper limit of the amount of $CoAl_2O_4$ formed after the first TPR is obtained when assuming that the metallic cobalt during TPO was oxidized to Co_3O_4, and the lower limit when it is assumed that the cobalt was oxidized to CoO. We thus calculated that the amounts of Co in the form of $CoAl_2O_4$ for the Co_4Rh and CoRh supported catalysts were 1.43–1.87 and 0.99–1.23 wt%, respectively. We feel that the upper limits are more realistic than the lower limits. For the monometallic catalysts we assumed the formation of Co_3O_4 and calculated 1.58 wt% Co in $CoAl_2O_4$. This indicates that the presence of the Rh does not prevent the formation of $CoAl_2O_4$ very much.

Having obtained an indication of the amount of $CoAl_2O_4$ present in the catalysts, one can calculate the dispersion of the truly metallic part of the catalyst. The results of this calculation are presented in the last column of Table 1 (upper limits for $CoAl_2O_4$ have been used). These results indicate that metal dispersion improves appreciably by adding Rh to Co. Since, as we shall see, the surface of Co–Rh particles is enriched in Co, this suggests a way of obtaining high Co dispersions.

Reduction of the oxidized monometallic cobalt is difficult (Fig. 4c) and incomplete at 773 K. The TPR profile is characterized by two peaks, one at about 600 K and the other at about 680 K. Comparison of the profile for bulk Co_3O_4 (Fig. 3a) with the one for

supported cobalt oxide indicates that also in the catalyst the reduction of Co_3O_4 is a sequential process. This result is in accordance with the TPR results reported by Paryjczak *et al.* (*16*). TPR experiments carried out in another TPR apparatus, in which higher final reduction temperatures could be reached, demonstrated that the temperature had to be raised to 1373 K in order to reduce the oxidized cobalt catalyst completely. Hydrogen was consumed to a great extent between 1073 and 1373 K probably caused by reduction of the surface $CoAl_2O_4$ spinel. The ratio of the hydrogen consumed during the second TPR and the oxygen consumed during the TPO preceding the TPR should be 2, because the oxygen consumed is converted to H_2O in the subsequent TPR. The values observed in the TPO and subsequent TPR run agree with this factor of 2 within the uncertainty of the measurements. This indicates that the oxidized cobalt formed during TPO was reduced completely during the subsequent TPR up to 773 K and that during TPO no new surface spinel $CoAl_2O_4$ was formed.

Reduction of supported Rh_2O_3 is complete by 400 K. The TPR profile is characterized by a single consumption peak around 363 K followed by desorption of H_2. The net H_2 consumption amounted to H_2/Rh = 1.52, indicating a reduction degree of rhodium after reduction of 100%.

The TPR profiles for the oxidized bimetallic Co–Rh/Al_2O_3 catalysts demonstrate that the reduction of cobalt oxide is catalyzed by the noble metal, rhodium. The maxima of the TPR profiles for the bimetallic catalysts are shifted toward higher temperatures in comparison with the monometallic rhodium catalyst: ΔT = 20 and 25 K for, respectively, CoRh/Al_2O_3 and Co_4Rh/Al_2O_3. Although the possibility of $CoRh_2O_4$ formation during TPO cannot be excluded, we are of the opinion that substantial $CoRh_2O_4$ formation is not likely because, first, the maximum oxidation temperature of 773 K during TPO is far below the formation temperature of bulk $CoRh_2O_4$ (T = 1073 K) and, second, on the basis of the TPR results of the bulk oxides we would have expected a peak around 500 K (cf. Fig. 3c). A shoulder around 500 K is observed in the TPR profile of Co_4Rh/Al_2O_3 and this shoulder may be assigned to $CoRh_2O_4$ or to cobalt oxide particles with a low rhodium oxide concentration. It is possible that during oxidation a segregation of both metal oxides has taken place and that after oxidation the oxides are not far apart from each other. In that way the very first formed rhodium may serve as a catalyst for the reduction. As in the case of Co/Al_2O_3, no significant amounts of $CoAl_2O_4$ were formed during TPO in the bimetallic catalysts, because the ratios of hydrogen consumed during the second TPR and oxygen consumed during TPO are within the experimental error equal to the theoretical value of 2.

The TPD profiles for the hydrogen-covered catalysts after the second TPR are presented in Fig. 4d. Note that the heating rate of 15 K min^{-1} is slow, so readsorption of hydrogen will take place and therefore no kinetic parameters for hydrogen desorption can be determined. Nevertheless, we used TPD to obtain information about the dispersion via the total amount of hydrogen desorbed. The TPD profile for Rh/Al_2O_3 is characterized by a main peak at 483 K and a shoulder at 300 K. Above 673 K hardly any hydrogen is desorbed. From the amount of hydrogen desorbed one can calculate a H/M_{TPD} value of 1.26, which is significantly lower than the value obtained by using the hydrogen chemisorption technique (H/M_{HC} = 1.53). We have to take into account that the H/M_{HC} value was obtained after a single reduction, and therefore the difference between the two values might be caused by sintering of rhodium during the TPO and subsequent TPR. The TPD profiles for the three cobalt-containing catalysts are characterized by two areas, one below 623 K which we assign to normal hydrogen desorption, and another above 623 K, which needs closer attention. Although the hydro-

gen adsorption energy for rhodium is reported to be higher than for cobalt, respectively, 113 and 100 kJ (*26*), our TPD's suggest the contrary. Even at 873 K desorption of hydrogen from cobalt was incomplete. Moreover, the total amounts of hydrogen desorbed largely exceeded the values calculated on the basis of the hydrogen chemisorption results. Therefore, we think that for the cobalt-containing catalysts the hydrogen detected above 623 K originated from another hydrogen source. It is obvious that this phenomenon only occurs in the presence of cobalt. We believe that dehydroxylation of the alumina support might play a very important role. It is known that alumina dehydroxylates above 673 K with the formation of water (*27*). Therefore, it is possible that during the TPD in the environment of the reduced cobalt crystallites the ratio of the partial pressures of water to hydrogen has become so high that the equilibrium $3\ Co + 4\ H_2O \rightleftharpoons Co_3O_4 + 4\ H_2$ is shifted to the right. This phenomenon has been reported previously by Schuit and de Boer (*28*) for Ni supported on SiO_2. A TPR to 773 K subsequent to a TPD of a cobalt catalyst did indeed show hydrogen consumption caused by reduction of cobalt oxide. However, the amount of hydrogen consumed was a factor of 2 lower than expected on the basis of the TPD results. We think that during TPD between 773 and 873 K, temperatures which had never been reached in the foregoing treatments, part of the oxidized cobalt was converted to the cobalt surface spinel $CoAl_2O_4$ which is not reducible below 773 K.

Up to now no direct information about the structure of the bimetallic crystallites could be obtained from the TPR results. Cobalt and rhodium are completely miscible (*13*) and therefore we assume that the regular solution model is valid, in which case thermodynamics predict that the metal with the lowest sublimation energy will be preferentially in the surface region of the alloy (*29*). The sublimation energy of cobalt is lower than that of rhodium and as a consequence surface enrichment of cobalt in the reduced Co–Rh particle is to be expected. From Extended X-Ray Absorption Fine Structure measurements we indeed found evidence for cobalt surface enrichment in supported bimetallic Co–Rh particles (*21*). When a bimetallic Co–Rh particle is exposed to oxygen at room temperature the cobalt enrichment in the surface will be even more pronounced because the interaction between oxygen and cobalt is stronger than that between oxygen and rhodium. This phenomenon is known as "gas-induced surface enrichment" (*30*). In order to demonstrate the surface enrichment of cobalt we recorded TPR profiles for the passivated catalysts (see Experimental). The profiles are presented in Fig. 5. The TPR profile for the passivated monometallic cobalt catalyst is characterized by a single peak around 513 K. On the assumption that during passivation oxygen is adsorbed dissociatively and that only the surface was

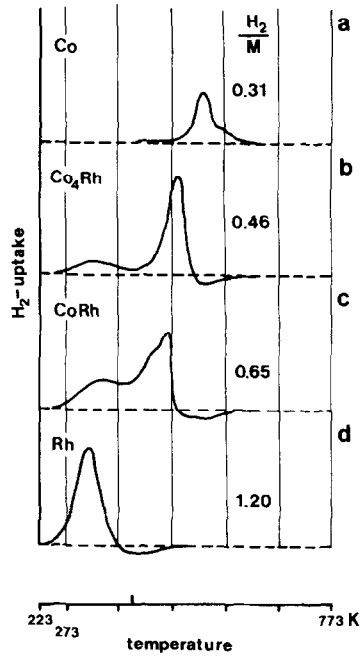

FIG. 5. TPR profiles for passivated alumina-supported catalysts. (a) Co (4.44 wt%), (b) Co_4Rh (4.57 wt%), (c) CoRh (5.40 wt%), and (d) Rh (2.30 wt%) catalysts.

covered by oxygen atoms with an $O/M_{surface}$ stoichiometry of 1, the dispersion determined from the amount of hydrogen consumed during TPR is 0.31. This value is much higher than the H/M value of 0.09 measured by hydrogen chemisorption. Therefore, the hydrogen consumed during TPR of the passivated Co/Al_2O_3 catalyst indicates that corrosive chemisorption had taken place during passivation.

The TPR profile for the passivated Rh/Al_2O_3 catalysts shows a single consumption peak around 300 K, followed by desorption of H_2. Passivation of this ultradispersed Rh catalyst has led to corrosive oxygen chemisorption, but not to full oxidation since the hydrogen consumption amounted to 1.20 H_2/M. Reduction of the passivated bimetallic Co_4Rh/Al_2O_3 catalyst occurs mainly in the temperature range 423–523 K, whereas a small shoulder is visible around 350 K. The maximum of the TPR profile is at about 483 K, only 30 K shifted to lower temperature compared to Co/Al_2O_3. Apparently, the presence of rhodium does not affect the reduction of the passivated cobalt as much as in the completely oxidized systems (cf. Fig. 4c). This can be explained by the assumption of covering of rhodium by cobalt oxide. Instead of the formation of the first rhodium metal atoms being the nucleation step, now the much more difficult formation of the first cobalt atoms is the nucleation step. The shift of 30 K might be caused by the presence of a few rhodium atoms in the surface. An X-ray photoelectron spectroscopy measurement confirmed that rhodium in the passivated Co_4Rh/Al_2O_3 catalyst is still mainly present as metallic Rh (binding energy of Rh $3d_{5/2}$ = 307.2 eV), which indicates that rhodium is hardly affected by oxygen. From the hydrogen consumed during reduction the total amount of oxidized cobalt can be calculated. On the assumption that the total amount of cobalt is oxidized to Co_3O_4 whereas rhodium is not affected, the theoretical H_2/M value is 16/15 (4 Co_3O_4 + 3 Rh + 16 $H_2 \rightarrow$ 16 H_2O + 3 Rh + 12 Co). However, from the 3.18 wt% cobalt 1.43–1.87 wt% has been lost as cobalt surface spinel. Thus the experimental H_2/M value of 0.46 must be compared with a theoretical value of 0.59–0.44, which indicates that cobalt was oxidized to a great extent during passivation. Thus, the passivated particles in Co_4Rh/Al_2O_3 consist of a rhodium-rich core and an outer shell consisting mainly of cobalt oxide. The shoulder around 350 K can be assigned to either bimetallic crystallites with a substantial amount of rhodium in the outer shell or to a rigorous passivation of small crystallites leading to the same situation as after a full oxidation. The structure of the TPR profile for the passivated $CoRh/Al_2O_3$ catalyst is similar to the profile for Co_4Rh/Al_2O_3 (Fig. 5c), although the shoulder is more pronounced and the main peak is shifted to lower temperatures. The latter indicates an increase of the rhodium concentration in the outer shell.

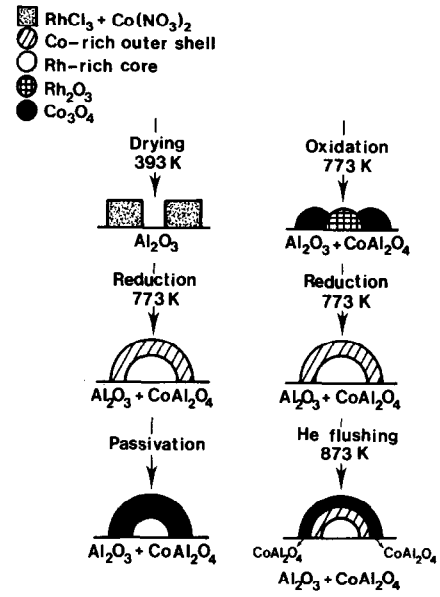

FIG. 6. Formation of bimetallic CoRh particles during reduction of the impregnated catalyst and the change in structure of the particles after different treatments.

All results obtained in the foregoing section have been rationalized by a model which represents the formation of bimetal-

lic Co–Rh particles supported on alumina and the change in structure of the particles after different treatments (cf. Fig. 6). After impregnation the metal salts are in intimate contact, as proven by the first TPR (Fig. 4a). During TPR bimetallic Co–Rh particles are formed, the outer shell of which is enriched in cobalt. Besides formation of Co–Rh particles, part of the cobalt reacts with alumina to produce $CoAl_2O_4$ which cannot be reduced below 773 K. When the reduced catalyst is exposed to oxygen, cobalt is oxidized to a great extent and the resulting cobalt oxide covers a rhodium-rich core. In this situation relatively high temperatures are needed to reduce the cobalt oxide because the covered rhodium cannot serve anymore as a reduction catalyst (Fig. 5b). A thorough oxidation of the catalyst induces a remodelling of the bimetallic particle in such a way that Rh_2O_3 is also exposed, so that a subsequent reduction is enhanced (Fig. 4c). During oxidation no new $CoAl_2O_4$ is formed. After reduction of the oxidized catalyst the bimetallic particles have been reformed. During the subsequent TPD the water formed by dehydroxylation of the alumina surface partly oxidizes cobalt and part of the oxide formed is converted to $CoAl_2O_4$.

ACKNOWLEDGMENTS

This study was supported by the Netherlands Foundation for Chemical Research (SON) with financial aid from the Netherlands Organization for the Advancement of Pure Research (ZWO). We are grateful to Dr. P. Arnoldy (University of Amsterdam) for performing some TPR measurements.

REFERENCES

1. Ponec, V., *Catal. Rev.-Sci. Eng.* **11,** 41 (1975).
2. Sinfelt, J. H., "Advances in Catalysis," Vol. 23, p. 19. Academic Press, New York, 1973.
3. Sachtler, W. M. H., *Catal. Rev.* **14,** 193 (1976).
4. Nakamura, M., Wood, B. J., Hou, P. Y., and Wise, H., *in* "Proceedings, 7th International Congress on Catalysis" Tokyo, 1980 (T. Seiyama and K. Tanabe, Eds.), Part A, p. 432. Elsevier, Amsterdam, 1981.
5. Bhasin, M. M., Bartley, W. J., Ellgen, D. C., and Wilson, T. P., *J. Catal.* **54,** 120 (1978).
6. Villeger, P., Barrault, J., Barbier, J., Leclercq, G., and Maurel, R., *Bull. Soc. Chim. Fr.* (1979), p. I-413.
7. Robertson, S. D., McNicol, B. D., de Baas, J. H., Kloet, S. C., and Jenkins, J. W., *J. Catal.* **37,** 424 (1975).
8. Jenkins, J. W., McNicol, B. D., and Robertson, S. D., *Chemtech* **7,** 316 (1977).
9. Wagstaff, N., and Prins, R., *J. Catal.* **59,** 434 (1978).
10. Paryjczak, T., Goralski, J., and Jozwiak, K. W., *React. Kinet. Catal. Lett.* **16,** 147 (1981).
11. Boer, H., Boersma, W. J., and Wagstaff, N., *Rev. Sci. Instrum.* **53,** 349 (1982).
12. Vis, J. C., van 't Blik, H. F. J., Huizinga, T., and Prins, R., *J. Mol. Catal.* **25,** 367 (1984).
13. Köster, W., and Horn, E., *Z. Metallkd.* **43,** 444 (1952).
14. Wood, J., Lindqvist, O., Helgesson, C., and Vannerberg, N. G., Eds., "Reactivity of Solids." Plenum, New York, 1977.
15. Brown, R., Cooper, M. E., and Whan, D. A., *Appl. Catal.* **3,** 177 (1982).
16. Paryjczak, T., Rynkowski, J., and Karski, S., *J. Chromatogr.* **188,** 254 (1980).
17. Hurst, N. W., Gentry, S. J., and Jones, A., *Catal. Rev.-Sci. Eng.* **24,** 233 (1982).
18. Vis, J. C., van 't Blik, H. F. J., Huizinga, T., van Grondelle, J., and Prins, R., *J. Catal.* **95,** 333 (1985).
19. Zowtiak, J. M., Weatherbee, G. D., and Bartholomew, C. H., *J. Catal.* **82,** 230 (1983).
20. Newkirk, A. E., and McKee, D. W., *J. Catal.* **11,** 370 (1968).
21. van 't Blik, H. F. J., Koningsberger, D. C., and Prins, R., *J. Catal.* **97,** 210 (1986).
22. van 't Blik, H. F. J., and Niemantsverdriet, J. W., *Appl. Catal.* **10,** 155 (1984).
23. Koningsberger, D. C., and Van Mill, L., in press.
24. Greegor, R. B., Lytle, F. W., Chin, R. L., and Hercules, D. M., *J. Phys. Chem.* **85,** 1232 (1981).
25. LoJacono, M., Shiavello, M., and Cimino, A., *J. Phys. Chem.* **75,** 1044 (1971).
26. Somorjai, G. A., "Chemistry in Two Dimensions: Surfaces," pp. 317 and 318. Cornell Univ. Press, London, 1981.
27. Knözinger, H., and Ratnasamy, P., *Catal. Rev.-Sci. Eng.* **17,** 31 (1978).
28. Schuit, G. C. A., and de Boer, N. H., *Recl. Trav. Chim. Pays-Bas* **70,** 1067 (1951).
29. Williams, F. L., and Nason, D., *Surf. Sci.* **45,** 377 (1974).
30. Bouwman, R., Lippits, G. J. M., and Sachtler, W. M. H., *J. Catal.* **25,** 300 (1972).